www.lepp.cornell.edu/public/CBN/2007/CBN 07-11
August, 2007

Emittance Growth Due to Space Charge Forces in an Electron Bunch Compressor

Richard Talman, Cornell Laboratory of
Elementary-Particle Physics
and
Nikolay Malitsky, Brookhaven National Laboratory

EMITTANCE GROWTH DUE TO SPACE CHARGE FORCES IN AN AN ELECTRON BUNCH COMPRESSOR

R. Talman, CERN, September 5, 2007

1. Review CTF–II Experiments
2. Puzzling features
   - dependence on bunch dimensions (to be stressed here)
   - CSR shielding, or lack thereof (will not be discussed)
3. Formulation of bunch evolution as intrabeam scattering (IBS) using the UAL string space charge formalism
4. Simulation of CTF–II results:
   - dependence of mean energy loss, energy spread, bunch length and emittances $\gamma\epsilon_x$ and $\gamma\epsilon_y$
   - on bunch charge, chicane settting R_{56} , distance along line, and bunch width (i.e on β_x)
5. "Standard Chicane"
   - Nominal, round beam; $\gamma\epsilon_x$= 1.0mm.mr, $\gamma\epsilon_y$= 1.0mm.mr
   - Ribbon (practical) beam; $\gamma\epsilon_x$= 1.0mm.mr, $\gamma\epsilon_y$= 0.01mm.mr
6. Conclusions
7. Computational practicalities

ABSTRACT. Using the UAL (Unified Accelerator Libraries) string space charge formulation, this paper simulates electron bunch compression results obtained at CTF-II, the CERN test facility for the "Compact Linear Collider". Allowing for inevitable configurational uncertainties, good agreement is found between theory and experiment. In particular, the simulation predicts a substantial dependence of horizontal emittance ϵ_x on beam width (as controlled by the lattice β_x-function) at the compressor location, consistent with the experimental observations. Previous simulations predict no such dependence. This dependence may be due to the centrifugal space charge force (CSCF), a current-dependent and position-dependent coherent transverse force.

The string space charge formulation avoids the regularization step (subtracting the free-space space charge force) which is required (to remove divergence) in other methods. This means that coherent synchrotron radiation (CSR) and CSCF as well as all free space, space charge forces are included. This is in contrast with theories of emittance growth that, ascribing the growth entirely CSR, break down at low energy.

Emittance growth in a "standard chicane" is also investigated. First to compare with other calculations—only modest emittance growth was observed, in agreement with previous determinations. Second, by comparing round and ribbon beams (like those actually needed in practice) to test whether the unexpected bunch shape dependence (described above) would give increased emittance for a 5 GeV beam as the beam height is reduced. (After correcting for halo generation, due to beam granularity in the simulation, and varying inversely with bunch height) the horizontal emittance, like both the momentum shift and the momentum spread, was found to be independent of bunch height. This is consistent with the emittance growth being dominated by CSR at high energy, as most workers have assumed.

PHYSICAL REVIEW SPECIAL TOPICS - ACCELERATORS AND BEAMS, VOLUME 3, 124402 (2000)

Emittance growth and energy loss due to coherent synchrotron radiation in a bunch compressor

H. H. Braun, R. Corsini, L. Groening, and F. Zhou
European Organization for Nuclear Research, CH-1211 Geneva 23, Switzerland

A. Kabel and T. O. Raubenheimer
Stanford Linear Accelerator Center, Menlo Park, California 94025

R. Li
Thomas Jefferson National Accelerator Facility, Newport News, Virginia 23606

T. Limberg
Deutsches Elektronen Synchrotron, D-22607 Hamburg, Germany
(Received 25 September 2000; published 13 December 2000)

Electron bunches of high charge (up to 10 nC) are compressed in length in the Compact Linear Collider Test Facility magnetic chicane to less than 0.4 mm rms. The short bunches radiate coherently in the chicane magnetic field, and the horizontal and longitudinal phase space density distributions are affected. This paper reports the results of beam emittance and momentum measurements. Horizontal and vertical emittances and momentum spectra were measured for different bunch compression factors and bunch charges. In particular, for 10 nC bunches, the mean beam momentum decreased by about 5% while the rms momentum spread increased from 2% to 8%. The experimental results are compared with simulations made with the code TRAFIC4.

PACS numbers: 29.27.Bd, 41.60.Ap, 41.75.Lx

PAC 2001

Recent Experiments on the Effect of Coherent Synchrotron Radiation on the Electron Beam of CTF II

L. Groening, M. Borland, H.H. Braun,
S. Doebert, A. Kabel

http://groening.home.cern/groening/csr_00.htm

- Introduction
- Experimental Setup at CTF II
- Effect of CSR Depending on :
  - Horizontal Beam Size
  - Height of Vacuum Chamber

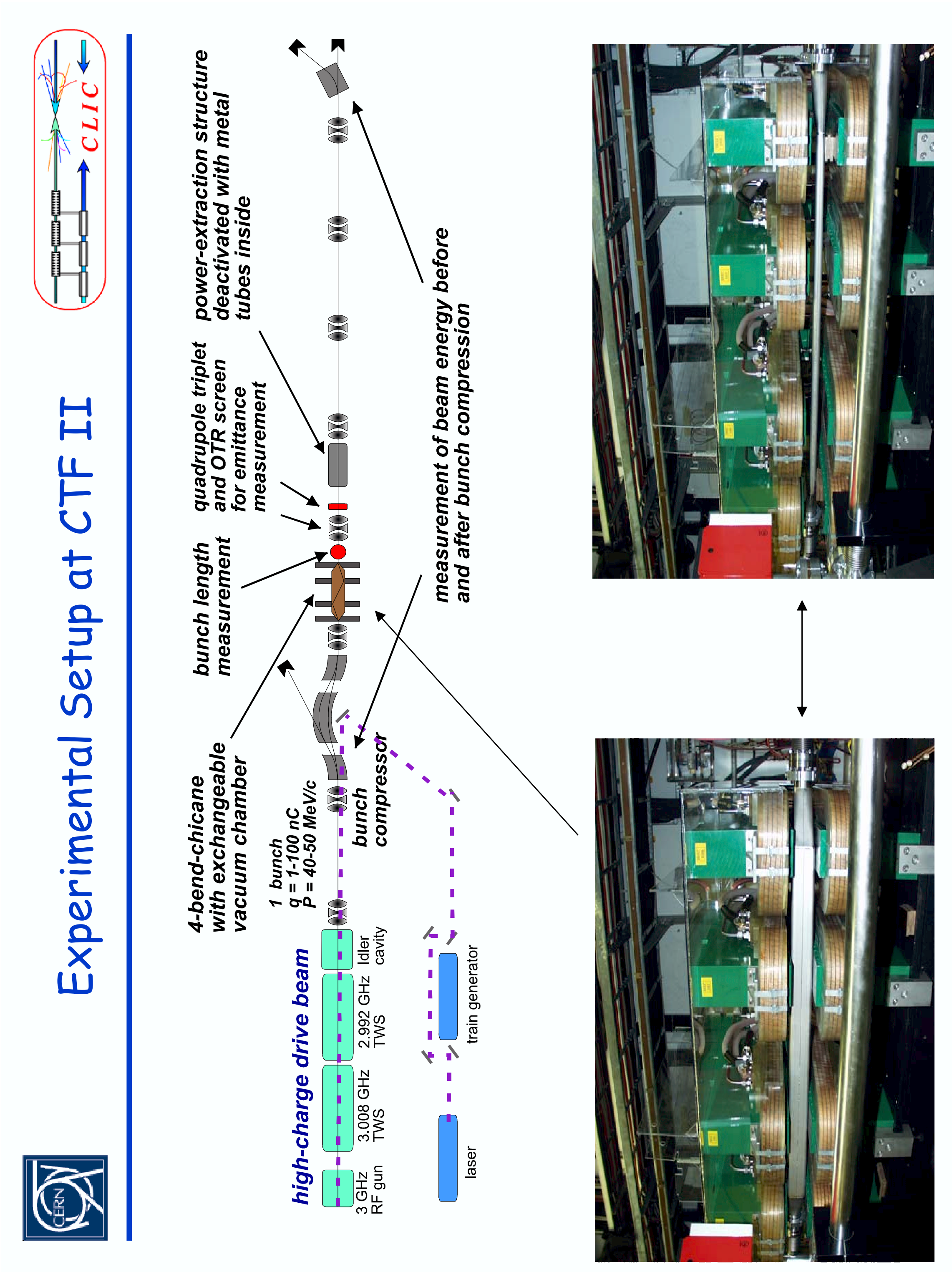

FIGURE 1. *CSR SHIELDING BY VACUUM CHAMBER WALLS WILL NOT BE DISCUSSED*

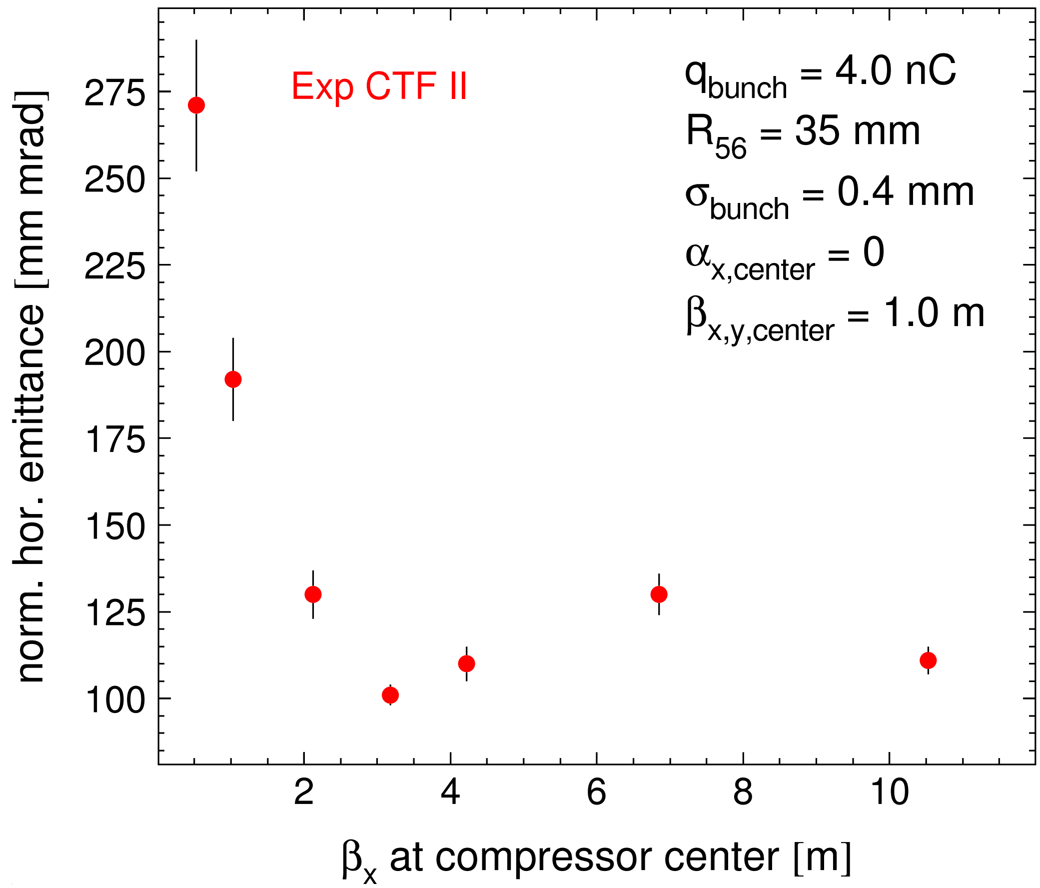
Exp CTF II
q_{bunch} = 4.0 nC
R_{56} = 35 mm
σ_{bunch} = 0.4 mm
$\alpha_{x,center}$ = 0
$\beta_{x,y,center}$ = 1.0 m
norm. hor. emittance [mm mrad]
275
250
225
200
175
150
125
100
2
4
6
8
10
β_x at compressor center [m]

Conclusion

- Experiment revealed strong growth of horizontal emittance for small hor. beam sizes in the bend
- Observation contradicts our understanding of emittance growth in bends and is not reproduced by simulations
- Result confirmed in various experiments at CTF II

- Measured energy loss agrees very well with simulations for the free space case
- Free space simulations fit also experiments for which significant shielding is expected
- Although predicted by simulations, no signs of shielding of CSR by conducting parallel plates were seen in our experiments

COMMENTS CONCERNING COHERENT SPACE CHARGE FORCES

CSR: "coherent synchrotron radiation"

- proportional to N^2
- can be worked out by integrating Poynting vector of far field
- OR, by evaluating self−work done by longitudinal self−force
- particles at head accelerate, particles at tail decelerate
- momentum deviation from local dispersion causes horizontal emittance growth
- requires "regularization" to suppress infinite self−work

CSCF: "centrifugal space charge force"

- transverse component of coherent space charge force
- proportional to N^2
- causes horizontal emittance growth the old−fashioned way, dependence of transverse force on transverse position
- often said to be neglible−−−more true at GeV energies

UAL: "Unified Accelerator Libraries"

- C++ port of diverse simulation codes to unified environment
- e.g. finite element tracking and space charge simulation

String Space Charge Model

- treats ALL (free space) space charge forces as IB scattering
- if the simulation had 10^{10} particles this would be perfect
- but simulation has, say, 1000 particles so Coulomb divergence causes erratic deflections of near encounters
- hence treat particles as longitudinally−aligned strings (needles) for calculating the e.m. fields they cause. Work in limit where strings are short compared to bunch length
- calculate retardation correctly −−− complicated !
- regularization is avoided
- scales poorly with N (as N^2), but OK for short beam line

STRING/POINT CHARGE REFORMULATION OF SPACE CHARGE FORCE

- Fundamental problem: Coulomb 1/r^2 and near collisions

- represent space charge force as force between point and ‘string’
- longitudinal force corresponds to coherent synchrotron radiation (CSR)
    - after regularization to remove (only logarithmic) divergence, self−work on bunch matches integrated Poynting power!
    - causes particle energy to depend on position along bunch, indirectly giving horizontal emittance growth
- transverse force is ‘‘centrifugal space charge force" (CSCF)
    - gives direct emittance growth

- formulation of space charge problem as ‘intrabeam scattering’
    - no regularization needed for numerical particle tracking
    - all space charge forces, Coulomb, Biot−Savart, CSR, CSCF are included
    - same simulation works at low and high energy

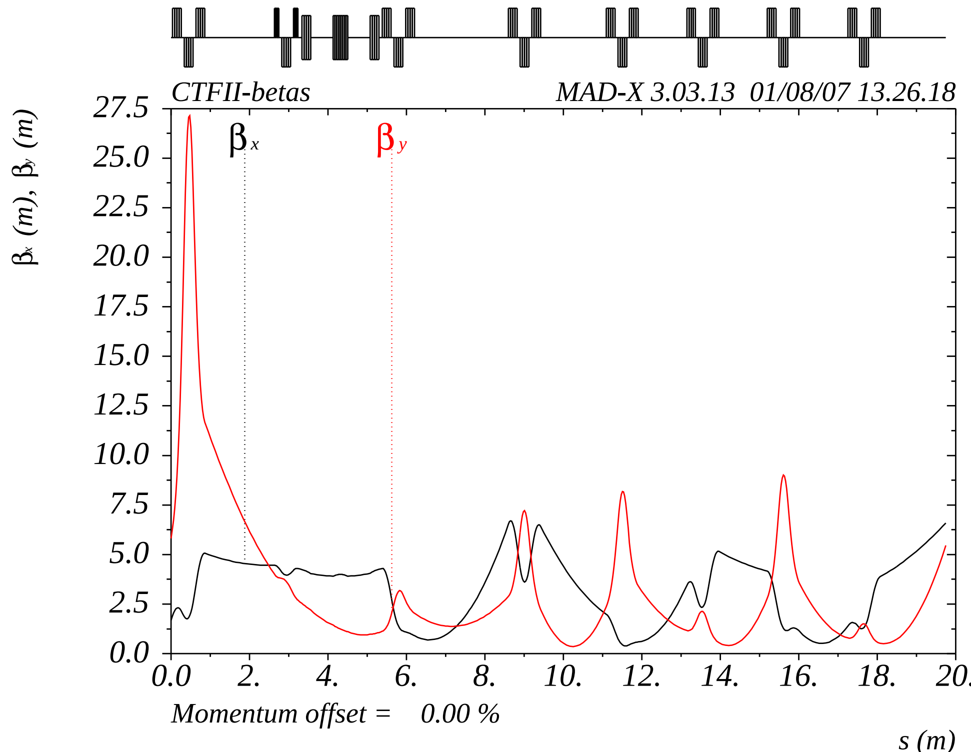

FIGURE 2. Beta functions for the CTF-II test facility (as reconstructed for $\beta_x = 4\,\text{m}$ for this report).

CLOSE TO, BUT NOT IDENTICAL TO, ORIGINAL OPTICS

Emittance vs. Hor. Beta Function

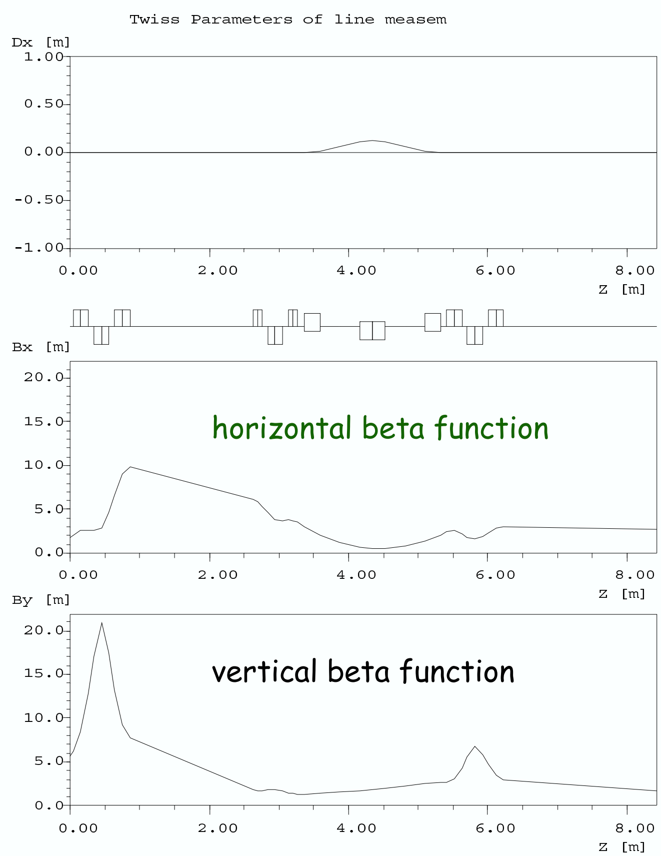

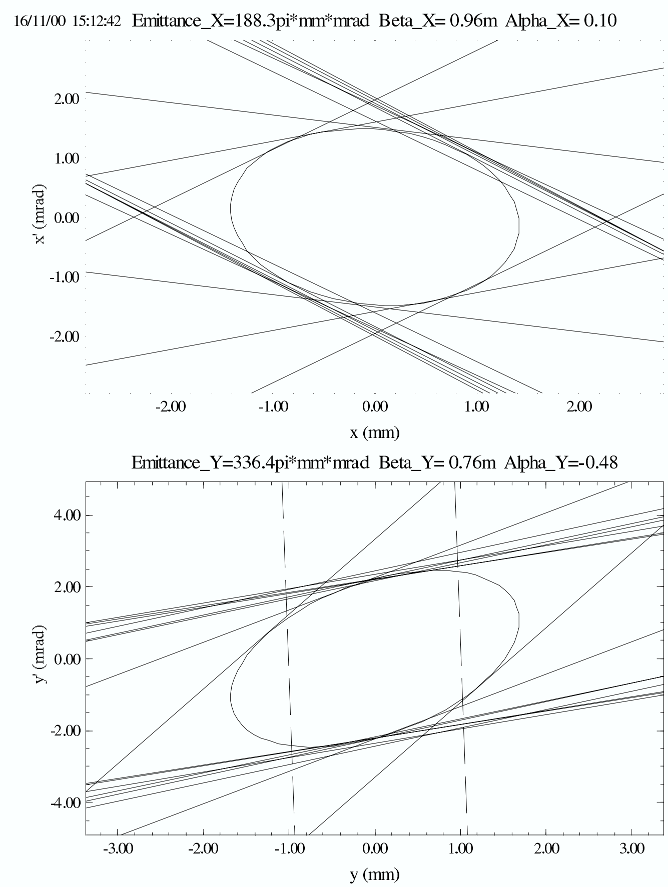

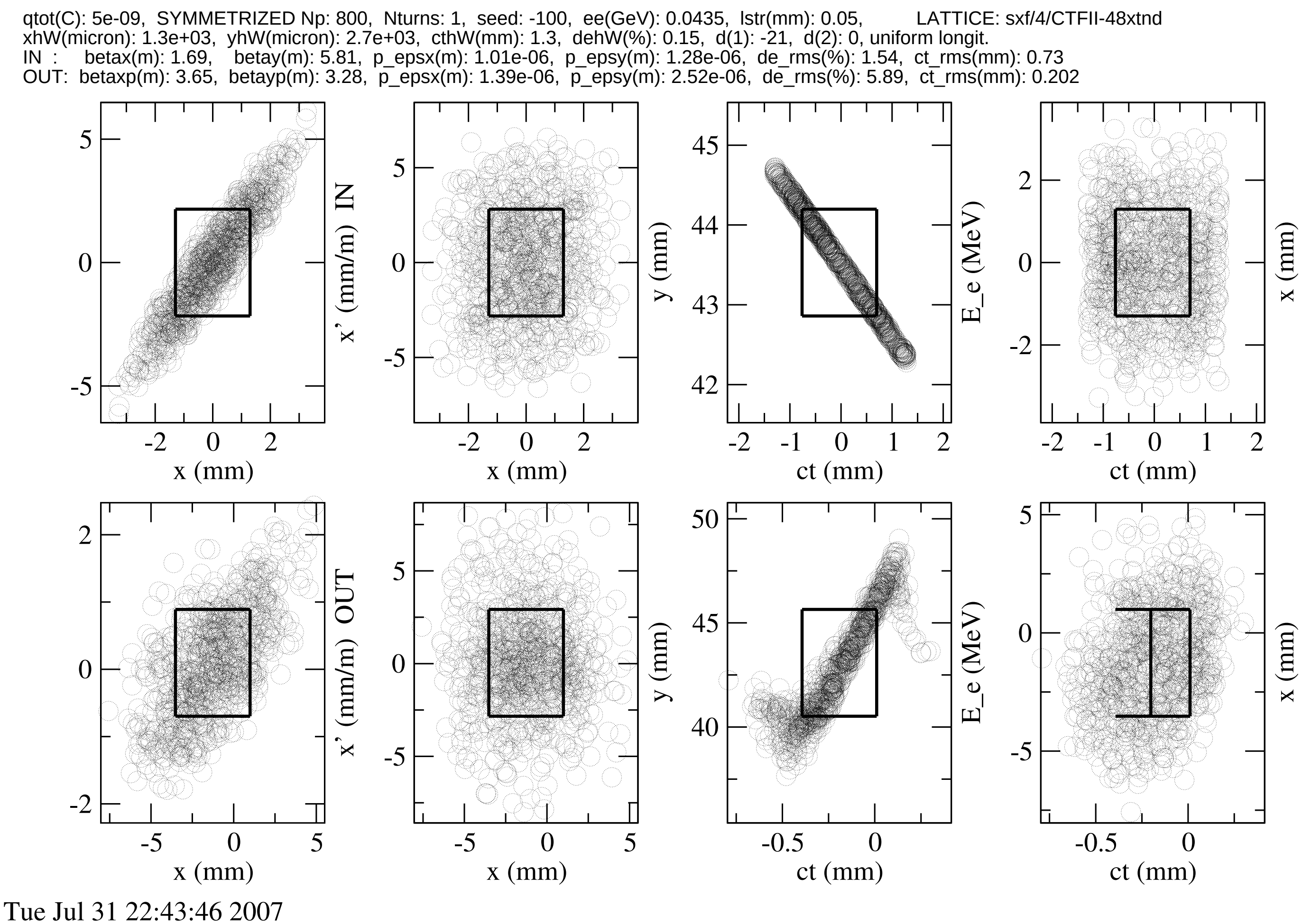

FIGURE 3. Particle distributions at the entrance and exit of CTF-II for $Q = 5\,\mathrm{nC}$, $R_{56} = 48\,\mathrm{mm}$. This is one of the extreme examples of (unexpected) growth of vertical emittance.

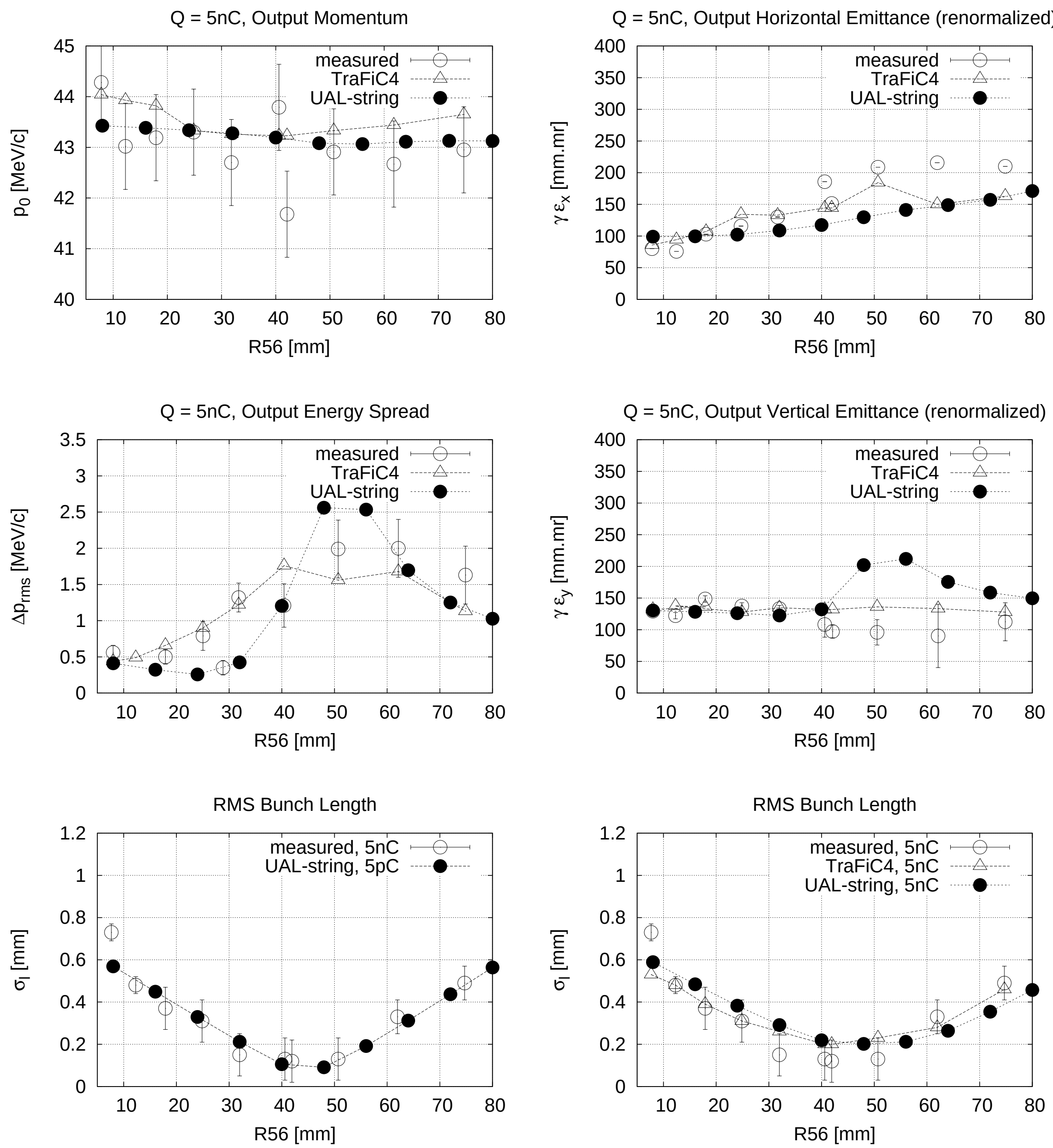

FIGURE 4. $Q = 5\,\mathrm{nC}$ output momentum, energy spread bunch length and emittances. The conversion from "raw" to "renormalized" is discussed in the text. In the bottom graphs the simulations predict a bunch length dependence on bunch charge Q near the minimum. The deviations visible in these graphs suggest that the system parameters (fit empirically without accounting for this dependence) may not be quite right. Is it possible the experimenters *tuned* to minimize the bunch length at the minimum at $Q = 5\,\mathrm{nC}$ rather than at $Q = 0$?

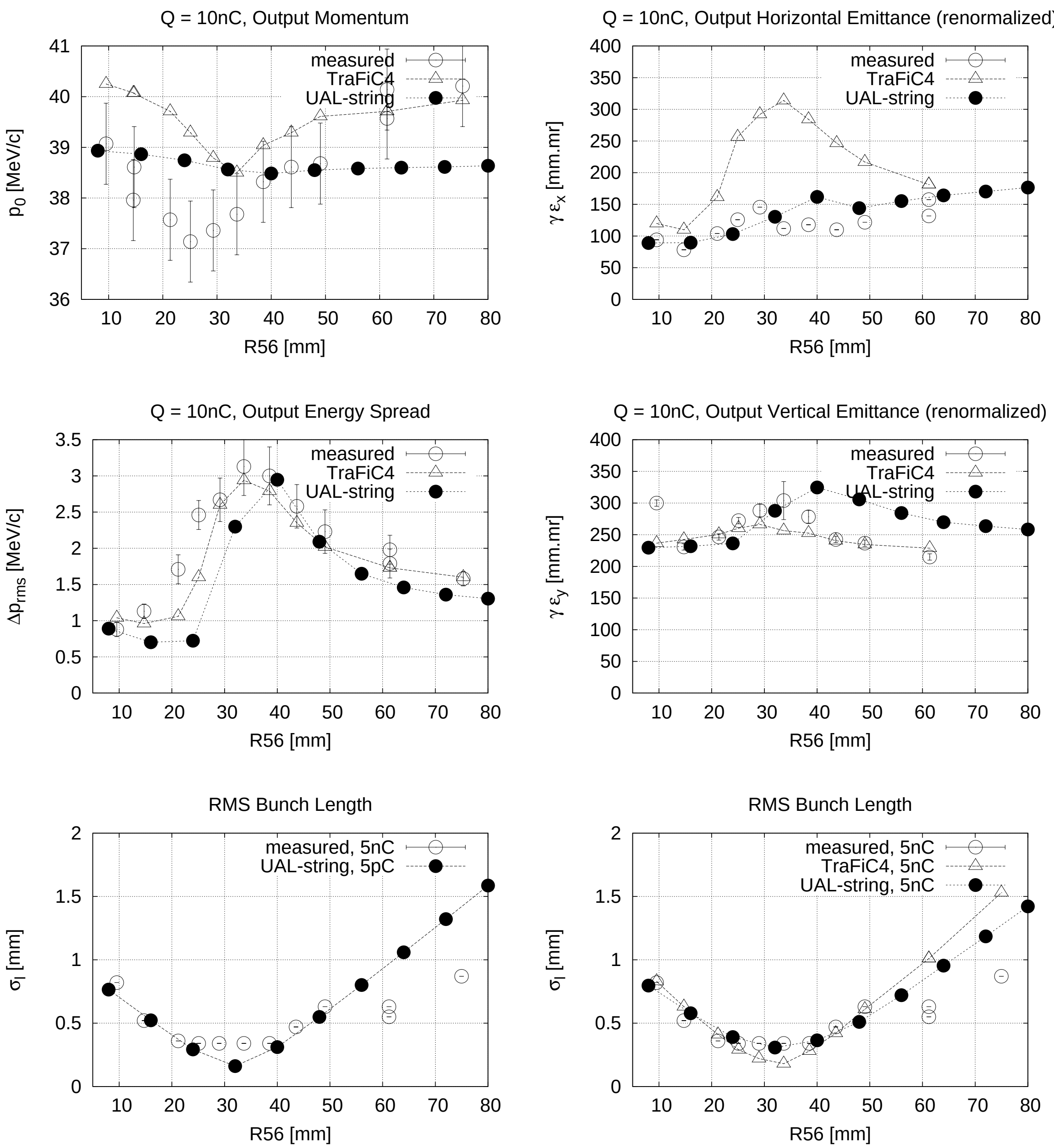

FIGURE 5. $Q = 10\,\mathrm{nC}$ output distributions. Deviations near the minimum were discussed along with the $5\,\mathrm{nC}$ data. These simulations used 800 particles, but results with 400 particles seemed essentially equivalent.

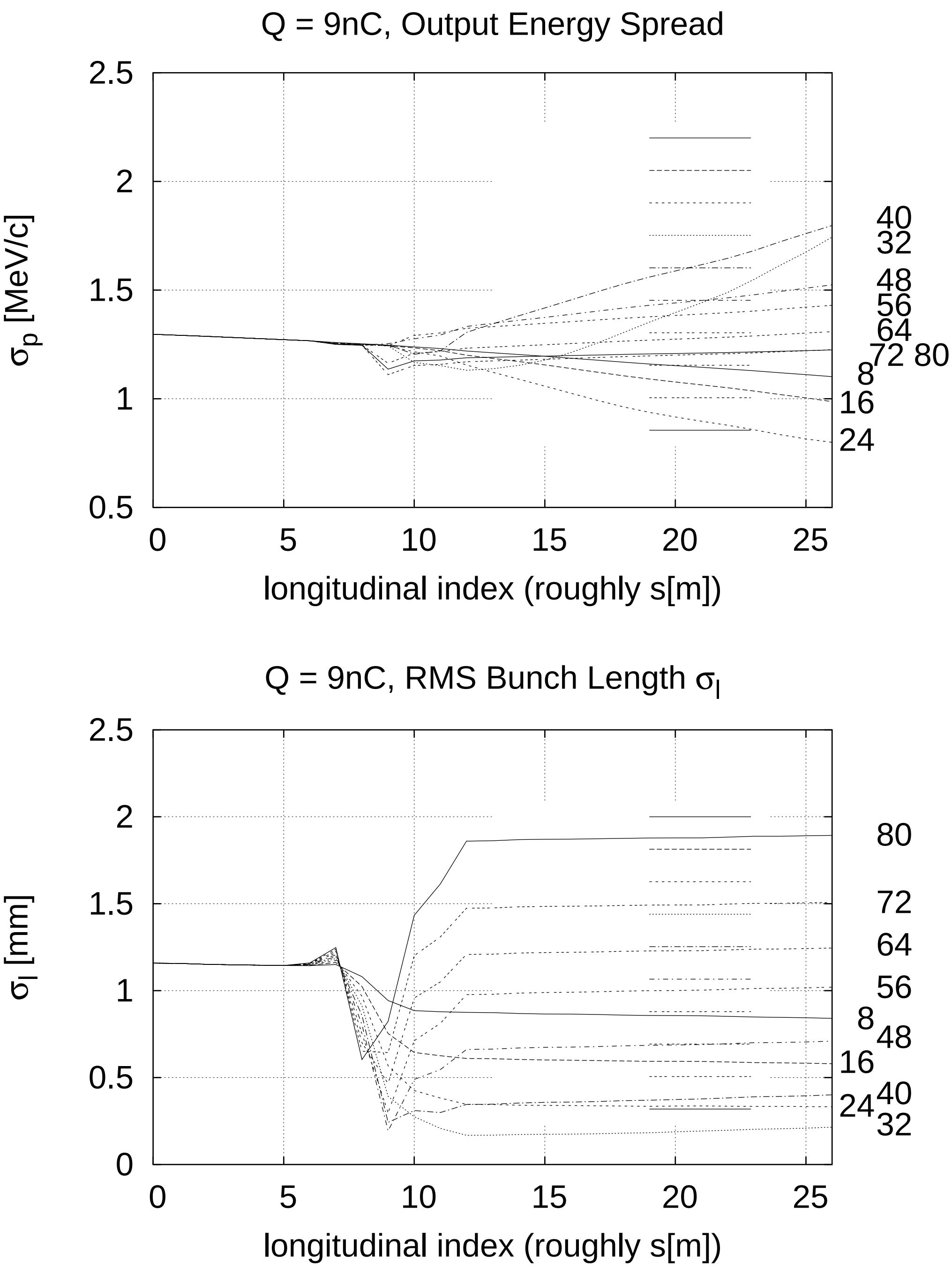

FIGURE 6. Dependence on longitudinal position of momentum spread Δp and bunch length σ_l. The chicane magnets are at index location 6, 8, 9, and 11 and other index locations are spaced more or less uniformly at 0.5 m intervals. Values of R_{56} are listed on the right.

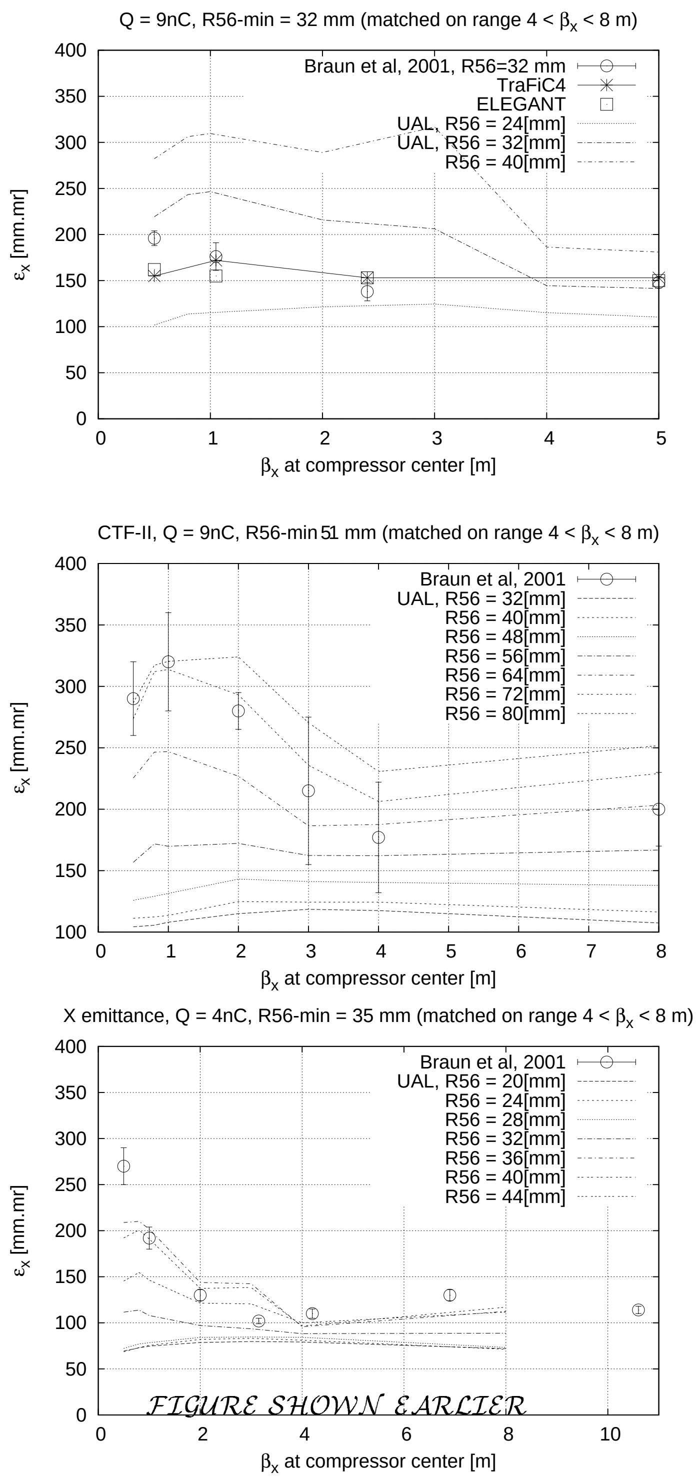

FIGURE 7. Measured and calculated dependence of horizontal emittance on β_x at chicane center for three different parameter combinations. Open circles are measured values, smooth curves are UAL string calculations. TraFiC4* and ELEGANT (upper graph only) simulations predict "no significant dependence on the beta function"[?].

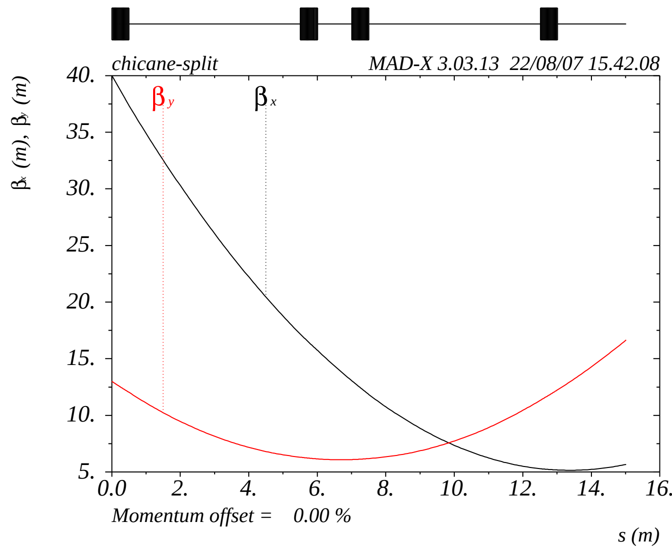

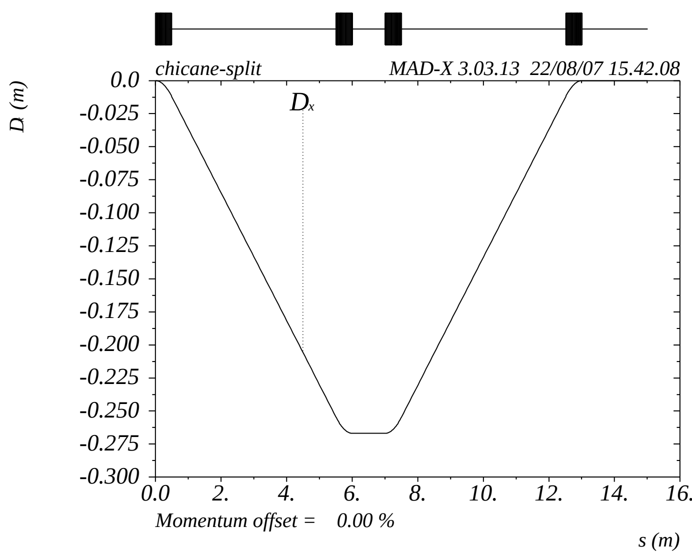

SIMULATION OF "STANDARD CHICANE"

(a) Nominal: "round beam"; $\gamma\epsilon_x = \gamma\epsilon_y = 1.0\,\text{mm.mr}$

(b) Needed in practice: "Ribbon beam": $\gamma\epsilon_x = 1.0\,\text{mm.mr}$, $\gamma\epsilon_y = 0.01\,\text{mm.mr}$

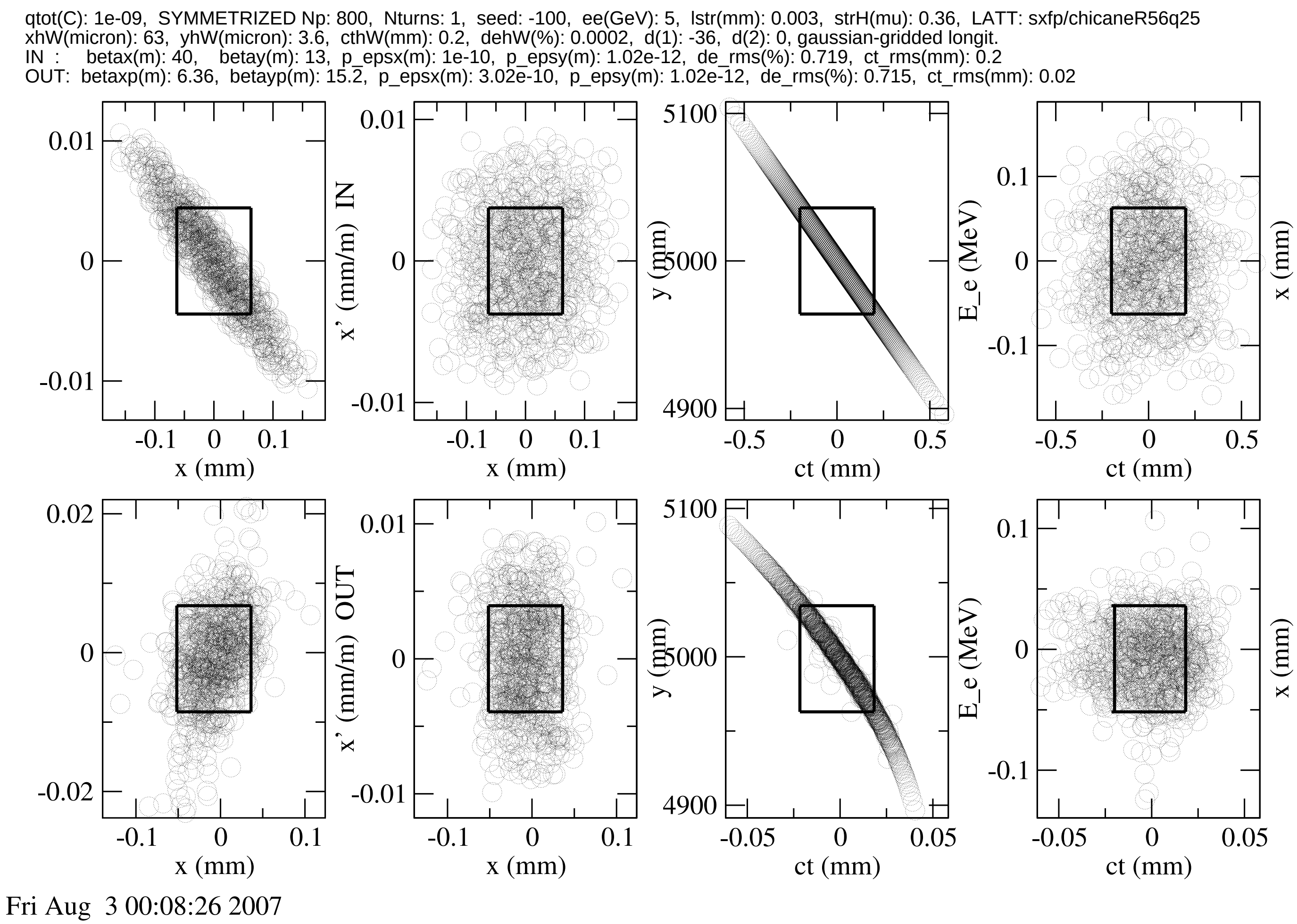

FIGURE 8. Particle distributions at the entrance and exit from the "standard chicane" benchmark;[?] However, to make the "halo" visible (in the bottom row, third plot over) the vertical emittance $\gamma\epsilon_y$ has been reduced to 0.01 mm.mr from its nominal value of 1 mm.mr.

TABLE 1. List of benchmarked codes giving the beam parameters at the output of the chicane (from Giannessi). Results in the bottom row are from the present simulation. The first term in the sums indicated by asterisks is ascribable to the "beam core". The second term is ascribable to the "beam halo" in the simulation, which is probably a numerical artifact coming from granularity in the beam. This emittance increase would, in any case, have little effect on luminosity in colliders or beam brilliance in x-ray sources. It is unclear whether a distinction between core and halo would be appropriate for any of the other entries in the table.

Dimension	Code Name	ΔE %	$\Delta\sigma_E$ %	$\gamma\Delta\epsilon_x$ mm.mr	$\gamma\Delta\epsilon_x$ $\epsilon_y = 0.01$mm.mr
3D	TRAFIC4	-0.058	-0.002	0.4	
3D	TREDI	-0.041	0.017	1.3	
3D	Program by Li	-0.056	-0.006	0.32	
1D Line charge	ELEGANT	-0.045	-0.0043	0.55	
1D Line charge	CSR_CALC	-0.043	-0.004	0.52	
1D Line charge	Program by Dohlus	-0.045	-0.011	0.62	
3D	UAL stringsc	-0.028	-0.0049	$(0.18 + 0.17)^*$	$(0.26 + 3)^*$?

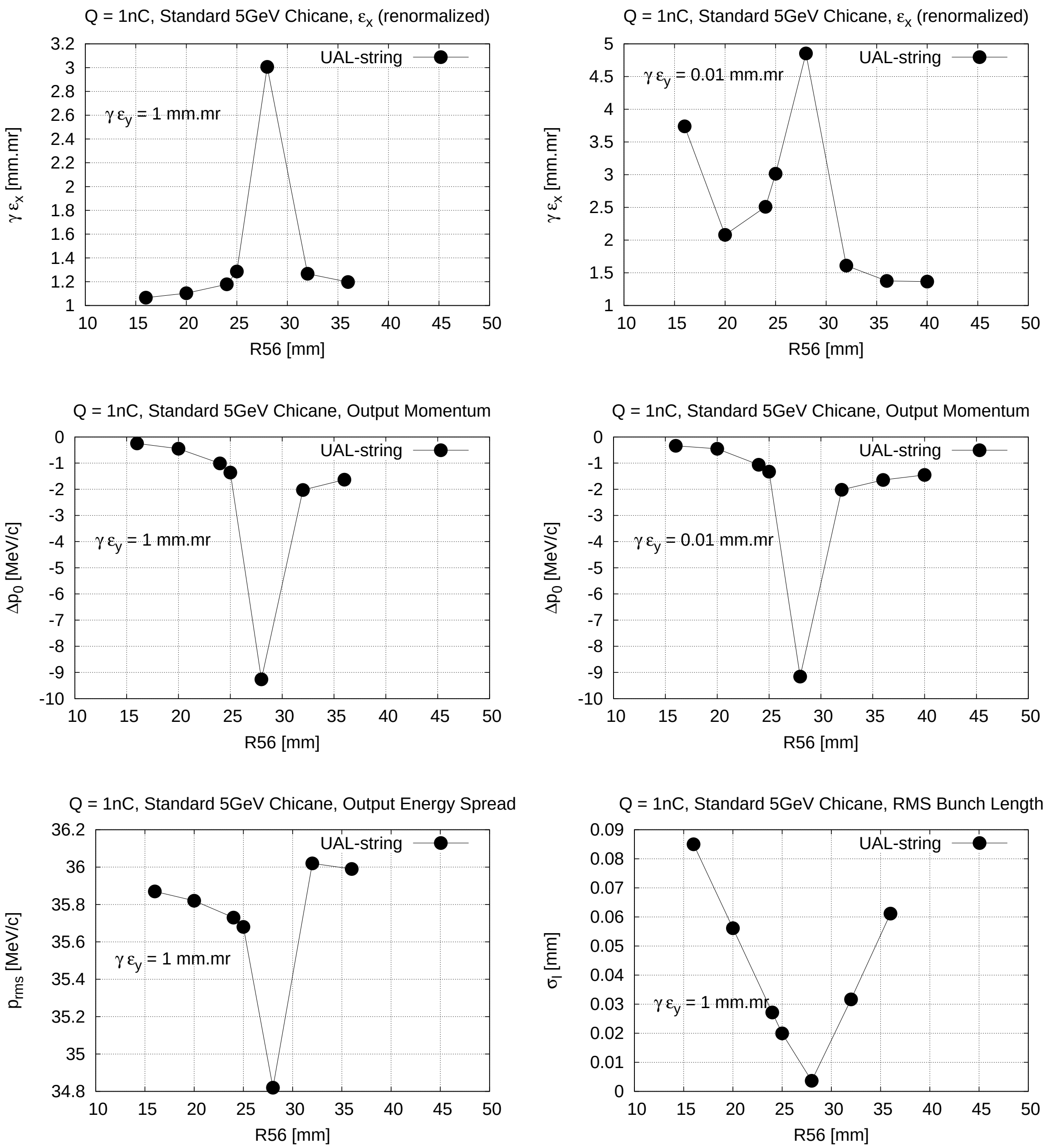

FIGURE 9. Dependence on R_{56} of various beam properties for round and ribbon beams. In all cases the electron bunch shape was Gaussian-gridded, the string length was $l_{\mathrm{str.}} = 3\,$micron, $\gamma\epsilon_{x0} = 1\,$mm.mr, $np = 800$, and $nsplit = 4$. Round beam, $\gamma\epsilon_y = 1\,$mm.mr, cases are shown on the left. The top two graphs on the right apply to the ribbon beam, $\gamma\epsilon_y = 0.01\,$mm.mr. As explained in the text, much of the horizontal emittance growth in the ribbon beam case is due to halo particles. The lower right figure shows bunch length for the round beam; the ribbon beam curve is essentially identical.

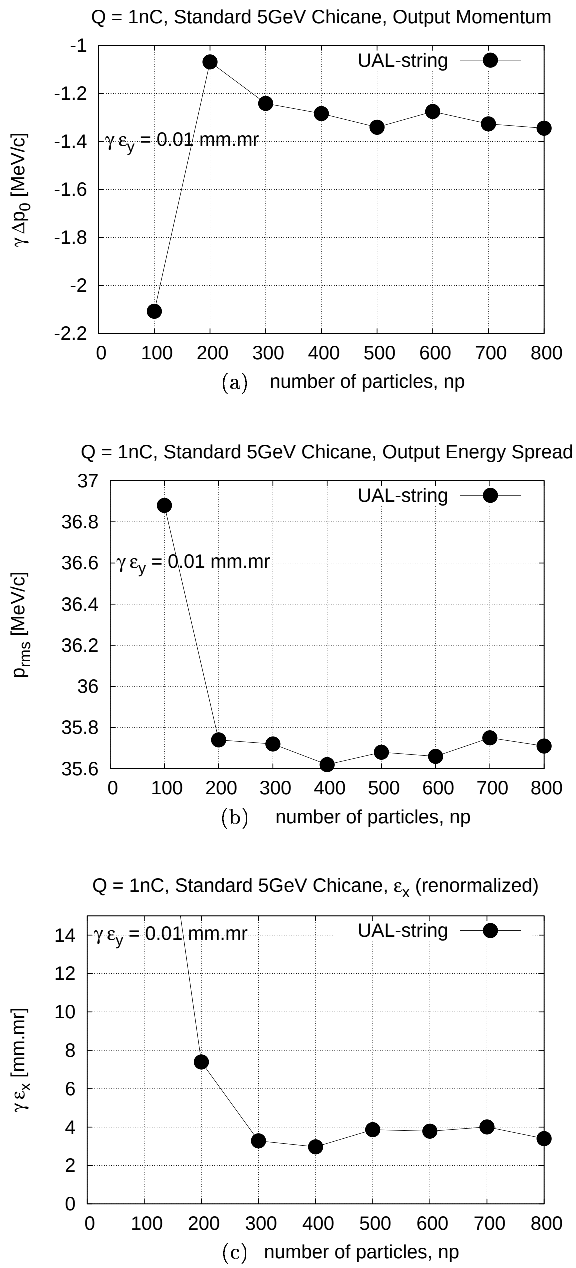

FIGURE 10. Dependence on the number of macroparticles, np, of various simulation outputs. In all cases $Q = 1\,\mathrm{nC}$, $R_{56} = 25\,\mathrm{mm}$, $\epsilon_{x0} = 1.0\,\mathrm{mm.mr}$, $\epsilon_{y0} = 0.01\,\mathrm{mm.mr}$ (ribbon beam). Round beam ($\epsilon_{y0} = 1\,\mathrm{mm.mr}$) plots are similar.

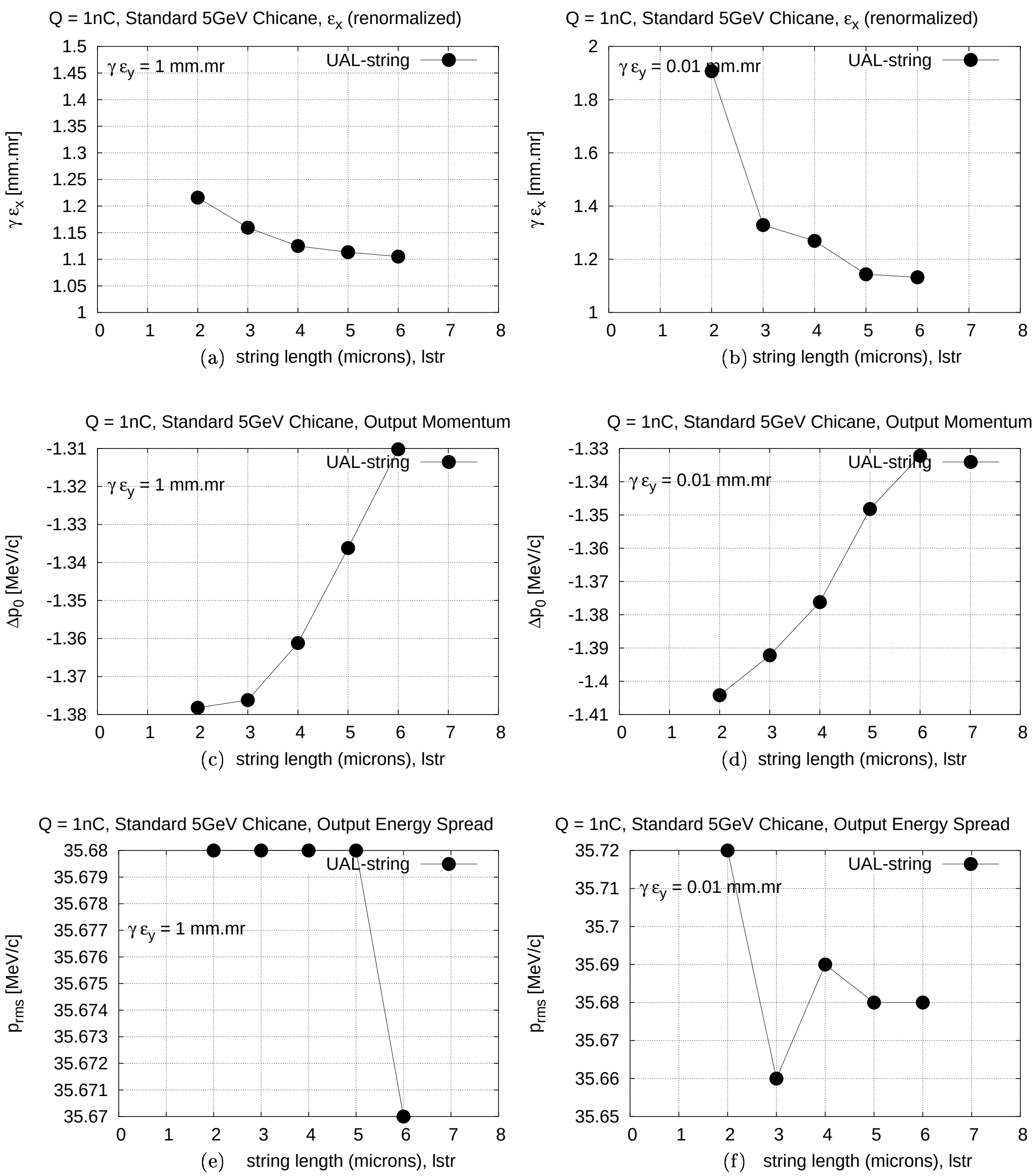

FIGURE 11. Dependence on the string length l_{str} for round and ribbon beams. In all cases $Q = 1\,\text{nC}$, $R_{56} = 25\,\text{mm}$ (giving $\sigma_{ct} = 20\,\text{microns}$), and $\gamma\epsilon_{x0} = 1.0\,\text{mm.mr}$, $np = 800$, and $nsplit = 16$, giving $1/(np.nsplit) = 0.078 \times 10^{-3}$ For the figures on the left, $\gamma\epsilon_{y0} = 1\,\text{mm.mr}$; for the figures on the right, $\gamma\epsilon_{y0} = 0.01\,\text{mm.mr}$.

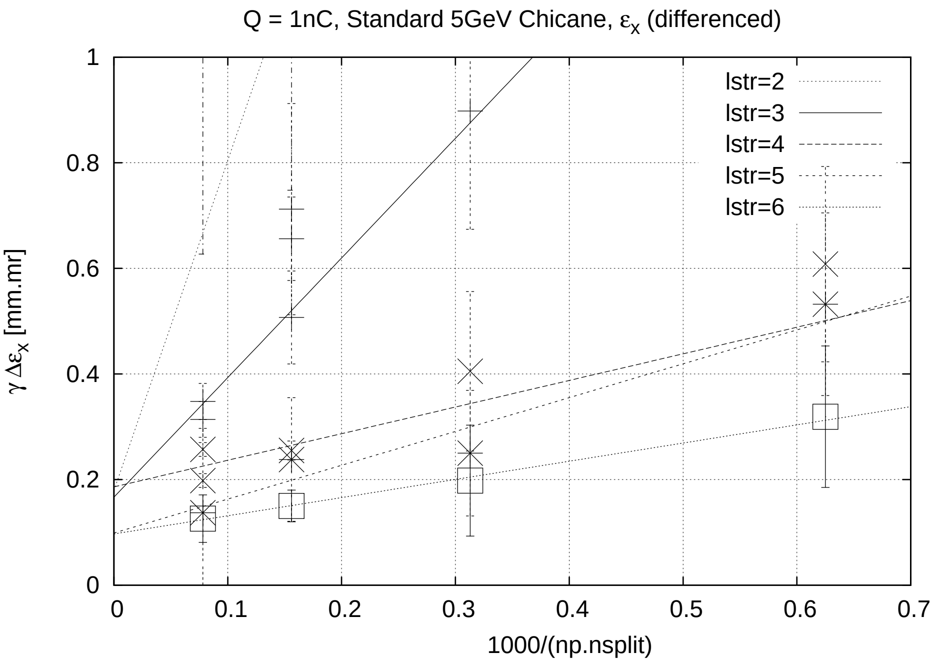

FIGURE 12. Dependence on $1/np/nsplit$ of the measured horizontal emittance growth $\gamma\Delta\epsilon_x$, for various values of string length $l_{\rm str}$, for a "ribbon" beam, with $\gamma\epsilon_y = 0.01$ mm.mr. For these simulations the string height $h_{\rm str} = yhW/10 = 0.36$ micron. Extrapolatation to the origin (infinitesimal charge per bunch) eliminates close-encounter halo production. Some residual dependence on $l_{\rm str}$ cannot be excluded but, in any case, it can be seen (comparing with Table 1) that reducing the beam height has not led to increased horizontal emittance growth.

yhW micron	$l_{\rm str}$ micron	n_p	$n_{\rm split}$	$1/(n_p n_{\rm split})$ $\times 10^{-3}$	δE MeV	$\delta\sigma_E$ MeV	$\gamma\epsilon_x$ (raw) mm.mr	$\gamma\epsilon_{x0}$ mm.mr	$\gamma(\epsilon_x - \epsilon_{x0})$ mm.mr
36	3(4)	800	8	0.156	-1.386±0.009	-0.2476±0.0037	1.165	0.981	0.183±0.019
	3(4)	800	4	0.313	-1.377±0.002	-0.2529±0.0020	1.145	0.967	0.177±0.059
	3(4)	800	2	0.625	-1.368±0.018	-0.2488±0.0090	1.333	0.982	0.351±0.155
3.6	3(4)	800	16	0.0781	-1.40±0.018	-0.243±0.002	1.330	0.982	0.348±0.087
	3(4)	800	8	0.156	-1.39±0.008	-0.234±0.010	1.372	0.996	0.441±0.101
	3(2)	1600	4	0.156	-1.43±0.014	-0.244±0.015	1.568	0.999	0.507±0.088
	3(4)	800	4	0.313	-1.40±0.016	-0.226±0.013	1.671	0.996	0.692±0.114
	3(4)	800	2	0.625	-1.39±0.059	-0.223±0.030	3.184	0.982	2.201±1.180
3.6	4(2)	800	16	0.0781	-1.38±0.01	-0.239±0.012	1.184	0.996	0.198±0.013

TABLE 2. Output bunch parameters for the standard chicane with nominal parameters. All beam measures except ϵ_x are essentially independent of all variables exhibited.

CONCLUSIONS

1. CTF−II, 40 MeV, simulation results agree quite well with experiment
   - CSR, though important, is not yet dominant
   - modest (fractional) growth of transverse emittance in most cases
   - less than fully−relativistic effects, Coulomb, Biot−Savart, and CSCF can account for
     - shrinkage/growth of vertical emittance
     - substantial growth of horizontal emittance as beam width is reduced

2. "Standard Chicane", 5 GeV, fair agreement among various simulations
   - CSR dominates
   - No growth of vertical emittance
   - Little (fractional) growth of horizontal emittance even with ribbon beam.

3. Treatment of bunch evolution as IBS using UAL string formulation is
   - computationally quick for short beam lines
   - subject to spurious "halo" generation, which can be suppressed by 1/N −> 0 extrapolation (and/or increased compute time)
   - in any case the halo would have little effect on luminosity/brillianc
   - bunch granularity would lead to true emittance growth
   - Touschek effect halo cannot be simulated (except using Piwinski formulas) but it is neglible in chicanes (though obviously not in rings, for short intense bunches)

$$\frac{1}{(a^2)^{3/2}} \to \left\langle \frac{1}{(\tilde{y}^2+a^2)^{3/2}} \right\rangle = \frac{1}{y_0} \int_0^{y_0} \frac{d\tilde{y}}{(\tilde{y}^2+a^2)^{3/2}} = \frac{1}{a^2} \frac{1}{(y_0^2+a^2)^{1/2}}$$

$$< \frac{1}{(y_0^2+a^2)^{3/2}}. \tag{1}$$

Assignment of height $strH = y_0$ to string. a is approximately the distance from point to string end. It is almost always large compared to y_0.

```
<apdf>
   <propagator id="stringsc" accelerator="ring">
      <create>
         <link algorithm="TEAPOT::DriftStringSCKick" types="Default" />
         <link algorithm="TEAPOT::DriftTracker" types="Marker" />
         <link algorithm="TEAPOT::DriftStringSCKick" types="Drift" />
         <link algorithm="TEAPOT::DipoleStringSCKick" types="Sbend" />
         <link algorithm="TEAPOT::MltStringSCKick"
                  types="Quadrupole|Sextupole|Multipole|[VH]kicker"/>
         <link algorithm="TEAPOT::RFCavityTracker" types="RfCavity"/>
         <link algorithm="TEAPOT::MltTracker" types="Kicker"/>
      </create>
   </propagator>
</apdf>
```

UAL APDF File Linking Simulation Methods to Element Types.

On a separate track, starting from a MAD-8 lattice description file, use a python script to translate it to MAD-X. Then run MAD-X to produce a (fully-instantiated) SXF lattice description file. The SXF file, which is input to the UAL space charge simulation, describes the lattice but has no reference whatsoever to the space charge calculation.

All space charge parameters (such as bunch charge and distributions) and directives (such as element splitting) is controlled in “main.cc” which provides the UAL procedural mechanism (and is intentionally ignorant of lattice details).